NUMERICAL INVESTIGATIONS OF FLUID STRUCTURE COUPLING: OSCILLATING HYDROFOIL

C. Münch[1], O.Braun[1], J.L- Kueny[2], F.Avellan[1]

[1] Laboratory for Hydraulic Machines, EPFL, Lausanne, Switzerland
[2] Laboratory of Geophysical and Industrial Flows, Grenoble, France
cecile.munch@epfl.ch
olivier.braun@epfl.ch
jl.kueny@hmg.inpg.fr
francois.avellan@epfl.ch

ABSTRACT

This paper presents an investigation of the hydro elastic behavior of vibrating blades in hydraulic machines, which is of strong interest for turbo machinery applications. As a representative case study for vibrating blade in hydraulic machines, a NACA 0009 oscillating hydrofoil is considered. The aim is to model the hydrodynamic moment acting on the oscillating hydrofoil. Two types of oscillation are investigated: forced and free motions. The fluid torque acting on the hydrofoil is modeled introducing an added moment of inertia, a fluid damping and a fluid stiffness coefficient. The model coefficients are identified through an investigation in the frequency domain of the forced motion. The influence of the frequency and the upstream velocity are investigated. The model is then validated in case of the free motion: numerical simulation and model prediction show good agreements in terms of frequency and dimensionless damping.

INTRODUCTION

Fluid structure interactions play an increasingly significant role in many engineering applications such as civil engineering, biomedical research, aerospace and turbo machines.

The aero elastic behavior of vibrating airfoil has motivated numerous experimental and numerical works. Carstens V. *et al.* (2003) investigate the aerodynamic damping in case of non linear fluid-structure interaction caused by oscillating shocks or strong flow separation. Gnesin V.I. *et al.* (2004) have developed an algorithm to investigate the mutual interaction between gas flow and oscillating blades. Park Jung Y.W. and Park S.O. (2005) investigate experimentally the unsteady characteristics of vortex shedding in the near wake of an oscillating airfoil. A numerical model for two dimensional flow around an airfoil undergoing prescribed heaving motions in a viscous flow has been proposed by Lewin G.C. and Haj-hariri H. (2003). Moffatt S. and He L. (2005) have developed two fully-coupled methods to predict the resonant forced response of turbomachinery blades. The case of a NASA Rotor 67 transonic aero fan rotor was investigated.

Interactions between water and structure have also be largely investigated, specially the case study of an oscillating cylinder. Govardhan R. and Williamson C.H.K. (2000) studied experimentally the transverse vortex-induced vibrations of an elastically mounted rigid cylinder in a fluid flow with the DPIV technique. Bishop R.E. and Hassan A.Y. (1964), measured the lift and drag forces in the case of a cylinder oscillating transversely, perpendicularly to the water stream. Ermanyuk E.V. (2000) studies experimentally the damped horizontal oscillations of a circular cylinder in linearly stratified fluid. One of the challenges in fluid structure interactions problems is to identify the added mass effect, damping effect and restoring force, see Brennen C.E. (1982), Rajasankar J. *et al.* (1993), Belanger F. *et al.* (1995), Han R.P.S. and Xu H. (1996), Conca C. *et al.* (1997), Khalak A. and Williamson H.K. (1997), Khalak A. and Williamson C.H.K. (1999), Ermanyuk E.V. (2000), Uchiyama T. (2003).

Despite their numerous industrial applications, very few studies have been devoted to the case of a hydrofoil. As a discovery experiment of fluid structure coupling in hydraulic machines, the flow around forced and free oscillating hydrofoil is numerically investigated. The hydrofoil represents one blade of the turbine (rotor or stator part) which can be exposed to unsteady dynamic force, like rotor stator interactions or strong flow separations. The present paper presents a model to predict the hydrodynamic action on the hydrofoil.

After a description of the hydrofoil motion, the computational details are exposed. Then the hydrodynamic moment modeling is investigated in the case of the forced motion. Finally, an assessment of the model is proposed in the case of the free motion.

NOMENCLATURE

Upstream Velocity	C_{ref}	$\left[\text{m} \cdot \text{s}^{-1} \right]$
Hydrofoil length	L	[m]
Hydrofoil thickness	e	[m]
Frequency	f	[Hz]
Non dimensional damping coefficient	ξ	[-]
Pulsation	ω	$\left[\text{rad} \cdot \text{s}^{-1} \right]$
Torque	T_f	[N·m]
Incidence angle	α	[rad]
Oscillation amplitude	α_0	[rad]
Moment of inertia	J_S	$\left[\text{kg} \cdot \text{m}^2 \right]$
Stiffness	k_S	[N·m]
Damping coefficient	μ_S	$\left[\text{kg} \cdot \text{m}^2 \cdot \text{s}^{-1} \right]$
Added moment of inertia	J_f	$\left[\text{kg} \cdot \text{m}^2 \right]$
Fluid stiffness	k_f	[N·m]
Fluid damping coefficient	μ_f	$\left[\text{kg} \cdot \text{m}^2 \cdot \text{s}^{-1} \right]$
Equivalent moment of inertia	J_e	$\left[\text{kg} \cdot \text{m}^2 \right]$
Equivalent stiffness	k_e	[N·m]
Equivalent damping coefficient	μ_e	$\left[\text{kg} \cdot \text{m}^2 \cdot \text{s}^{-1} \right]$
Natural pulsation	ω_o	$\left[\text{rad} \cdot \text{s}^{-1} \right]$

SIMULATIONS

Case Study

The 2D hydrofoil, of NACA 0009 type, has a chord length of 100mm, a thickness of 9.7mm and a blunt trailing edge, see Figure 1.
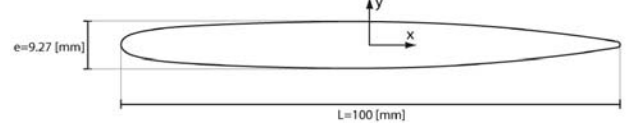

Figure 1 NACA 0009 Hydrofoil with rounded trailing edge.

Two types of motions are considered: forced and free oscillations. In both cases, the hydrofoil rotates around its center of gravity.

In the forced motion case, see Figure 2, the incidence angle, α(t), is defined as a periodic function of time by equation (1).
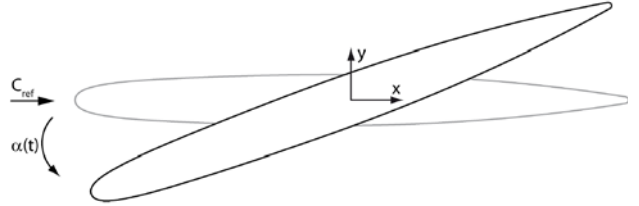

Figure 2 Sketch of the forced oscillating case.

$$\alpha(t) = \alpha_o \sin(\omega t) \qquad (1)$$

The oscillation amplitude α_o and the pulsation ω are forced.

The free motion case consists of a 1-degree-of-freedom model of an oscillating hydrofoil, see Figure 3. The hydrofoil is attached to a flexible structure featuring a given stiffness and a damper. The structural parameters of the 2D hydrofoil are thus the momentum of inertia J_S, the stiffness k_S and the damping coefficient μ_S. The hydrofoil is departing at rest from an incidence angle α_o. The free oscillating motion of the hydrofoil is simulated. The initialization phase is achieved in three steps: (i) setting up the hydrofoil at the initial incidence α_o during N_1 iterations. (ii) Simulating the flow in this stationary position during N_2 iterations. (iii) Starting up the oscillations of the profile. A Fortan program is implemented in CFX to solve the free motion. The balance of the angular momentum is used to calculate the new incidence of the hydrofoil as a function of the torque,

2

rotational velocity and incidence at the previous time step, see equation (2).

$$\alpha^{n+1} = \alpha^n \left(2 - \frac{\mu_s}{J_s}\Delta t - \frac{k_s}{J_s}\Delta t^2 \right) + \alpha^{n-1}\left(\frac{\mu_s}{J_s}\Delta t - 1 \right) + \frac{\Delta t^2}{J_s}T_f^n \quad (2)$$
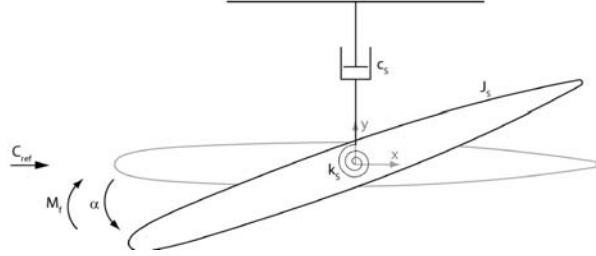

Figure 3 Sketch of the free oscillating case.

Numerical Methods

The numerical unsteady simulations are carried out with ANSYS CFX 10 ®. This code, based on finite volume methods, solve**s** the incompressible Unsteady Reynolds Averaged Navier-Stokes (URANS) equations in their conservative form and the mass conservation equation. The set of equation is closed with a two equations turbulence model: the Shear Stress Transport (SST) model, see Launder B.E. and Spalding D.B. (1974), Wilcox D. (1993), Menter F.R. (1994). The discretization of the equations is made with the Backward Euler implicit scheme, second order in time, and an advection scheme with a specified blend factor equal to one corresponding to a second order in space.

The numerical parameters are summarized in Table 1. For further details, the reader can refer to the manual of ANSYS CFX (2005)

Table 1 Numerical parameters

Simulation type	Spatial scheme	Temporal scheme	Time step	Turbulence model
Unsteady	2nd order	2nd order	t=T/480	SST

Since the hydrofoil is oscillating around the center of mass, the moving mesh approach is used. The motion of the hydrofoil wall is specified and the mesh is deformed to follow this motion. The moving mesh approach allows to diffuse the displacements applied on boundaries to other mesh points by solving a mesh displacement diffusion equation. The mesh deformation is characterized by a mesh stiffness, Γ_{disp}, defined by equation (3) .

$$\Gamma_{disp} = \frac{1\,[m^3 \cdot s^{-1}]}{\text{Wall distance}} \quad (3)$$

The hydrofoil is placed in a rectangular computational domain: $250mm \times 150mm$. The mesh consists of a structured grid of 40'000 nodes, see Figure 4. For computational reason, a thickness is needed is the third direction: b=1mm discretized by two nodes.
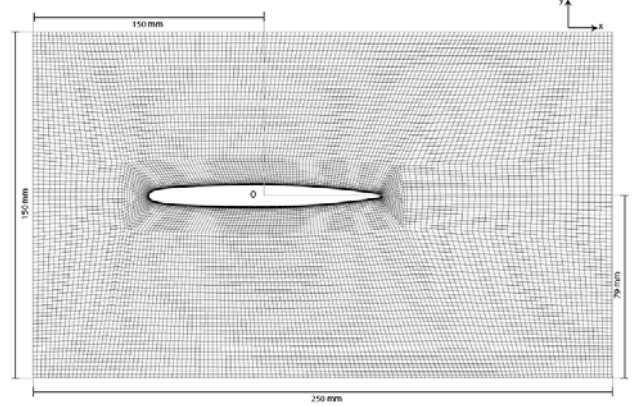

Figure 4 Computational domain.

The characteristics of the computational domain are summarized in Table 2.

Table 2 Characteristic of computational domain

Mesh type	Nodes	Min. Face Angle	Max. y^+
structured	40'000	38°	5

The boundary conditions are:
- Upstream: uniform velocity $\vec{C}_{ref} = C_{ref}\vec{x}$;
- Outlet: constant average static pressure $p = p_{out}$;
- Hydrofoil wall: non slip;
- Top and bottom of the computational domain: symmetry conditions.

Grid and Time Step Independancy

The fluid torque amplitude in the case of the forced oscillating hydrofoil, $C_{ref} = 10 \; m \cdot s^{-1}$ and f=100Hz is considered to test the grid and time step influence. The finer mesh and the smaller time step are respectively considered as reference, and the value plotted is defined by equation (4).

$$T_{diff} = \left| \frac{T_f - T_{ref}}{T_{ref}} \right| \quad (4)$$

Three different meshes are defined in Table 3.

3

Table 3 Characteristic of the three meshes.

	Coarse	Medium	Fine
Nodes	20'000	40'000	60'000

According to the difference of less than 0.3 % between the finer and the medium mesh, see Figure 5, the medium mesh is selected.
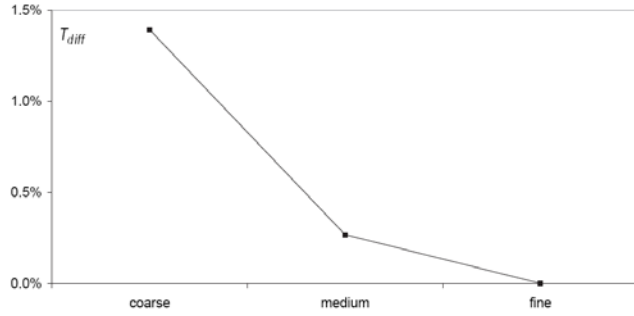

Figure 5 Grid independence test.

Then, three different time steps are tested, see Table 4.

Table 4 Characteristic of the three time steps.

	Large	Medium	Small
Iterations per period	120	480	1920

According to a difference of less than 0.3 % between the smaller and the medium time steps, see Figure 6, the medium time step is selected.
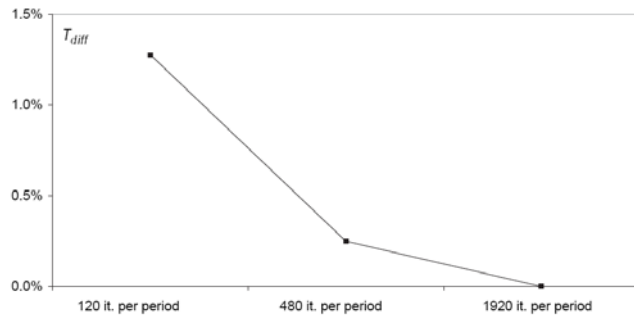

Figure 6 Time step impendence test.

HYDRODYNAMIC ACTION MODELING

Model

The hydrodynamic moment acting on the hydrofoil is assumed to result from the following moments:

- inertial moment as the product of added moment of inertia, J_f and the angular pitching acceleration $\ddot{\alpha}$; it represents the action of the flow mass oscillating with the profile;
- damping moment as the product of the damping moment coefficient μ_f and the angular velocity $\dot{\alpha}$, resisting the motion;
- restoring moment, given as the product of a stiffness moment coefficient k_f and the rotation angle α, which can either tends to bring the body back to or move it away from the reference position.

$$T_f = -(J_f\ddot{\alpha} + \mu_f\dot{\alpha} + k_f\alpha) \qquad (5)$$

Identification of the Model Parameters

The three coefficients can be assumed to depend on the fluid velocity and the frequency of the oscillation. The simulations of the forced oscillating hydrofoil are used to determine J_f, k_f and μ_f. The fluid parameters are identified with an investigation of the fluid torque in the frequency domain. The case study of a forced oscillator is described by a transfer function between an input, the exciting moment to force the motion, and an output, the resulting motion. In these simulations, the output is imposed: $\alpha(t) = \alpha_o \sin(\omega t)$. For the input, the resulting fluid torque on the profile, T_f, is computed taking into account the pressure and the friction forces. Indeed, the part of the viscous friction is very small as compared to the pressure term, around 1%. The transfer function, defined as the ratio between the output and the input, is calculated as:

$$H = \frac{\alpha}{T_f} \qquad (6)$$

The solution searched is of type $\alpha(t) = \alpha_o e^{i\omega t}$, the transfer function can be written as:

$$H(\omega) = \frac{1}{J_f\omega^2 - k_f - i\mu_f\omega} \qquad (7)$$

The magnitude and the phase as a function of the pulsation are represented in Figure 7.
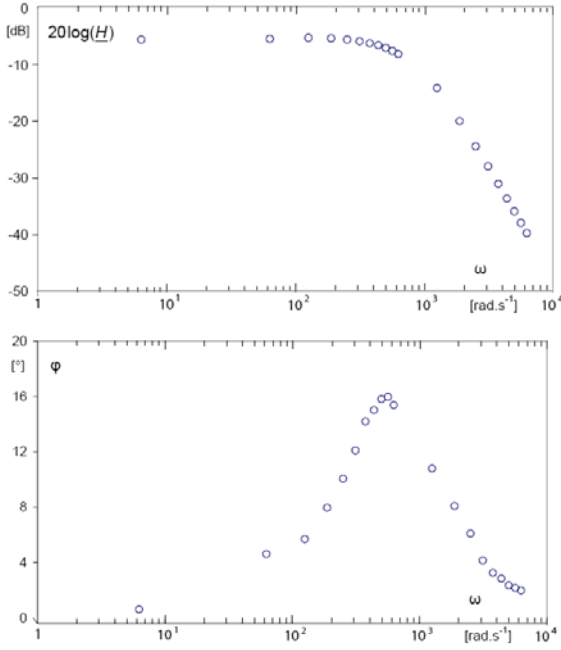
4

Figure 7 Magnitude and phase of the transfer function in case of forced motion

- Identification of J_f

The unknown J_f is identified with an asymptotic matching in the Bode diagram. Indeed for high pulsations, the transfer function modulus behaves like:

$$\lim_{\omega \to \infty} \underline{H}(\omega) = \frac{1}{J_f \omega^2} \qquad (8)$$

- Identification of μ_f

The fluid damping is identified through the imaginary part of the transfer function, see equations 9 to 11.

$$\text{Im}(H) = \underline{H} \sin \varphi \qquad (9)$$

$$\text{Im}(H) = \underline{H}^2 \mu_f \omega \qquad (10)$$

$$\mu_f = \frac{\sin \varphi}{\underline{H}\omega} \qquad (11)$$

- Identification of k_f

The stiffness moment coefficient is identified through the reel part of the transfer function, see equations 12 to 14.

$$\text{Re}(H) = \underline{H} \cos \varphi \qquad (12)$$

$$\text{Re}(H) = \underline{H}^2 \times \left(J_f \omega^2 - k_f \right) \qquad (13)$$

$$k_f = J_f \omega^2 - \frac{\cos \varphi}{\underline{H}} \qquad (14)$$

RESULTS

Influence of the frequency and the upstream velocity

In Figure 8, the dimensionless transfer function magnitude, defined by equation (15), is represented in the Bode diagram for three values of the upstream velocities as a function of the Strouhal number defined by equation (16). With this normalization, the transfer functions of all the investigated cases fit well.

$$\underline{H}^* \left(f^* \right) = \frac{H\left(f^* \right)}{\underline{H}_{15}(0)} \times \frac{C_{ref}^2}{15^2} \qquad (15)$$
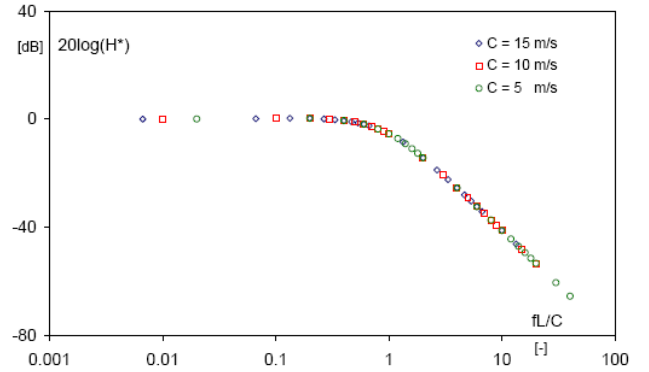
$$f^* = \frac{fL}{C_{ref}} \qquad (16)$$

Figure 8 Bode Diagram: Results for three values of the upstream velocity

In Figure 9, the value of J_f is given for four values of the upstream velocity. A very small variation is observed. According to this result, J_f can be assumed to be independent of the upstream velocity as found by Brennen C.E. (1982). The value of J_f calculated with the potential flow analysis, equation (22), represented in blue in Figure 9, corroborates to the values calculated with the numerical simulations.
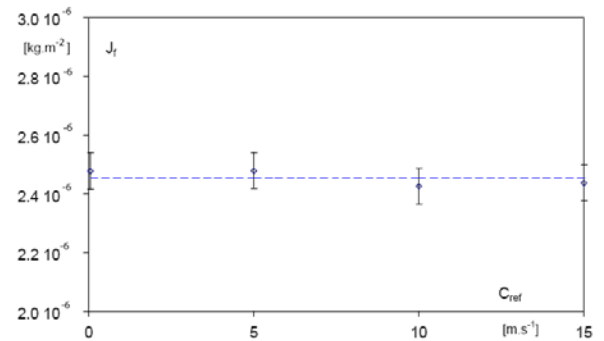

Figure 9 Influence of the upstream velocity on the added moment of inertia

5

$$J_f^* = \frac{1}{8}\rho\pi\left(\frac{L}{2}\right)^4 e \tag{17}$$

$$J_f^* = 2.45 \ 10^{-6} \ [kg \cdot m^2]$$

Then the influence of the frequency and the upstream velocity on the fluid damping is investigated. To normalize this coefficient, the normalization of the fluid torque is used, see equation (17).

$$T_f^* = \frac{T_f}{\rho \dfrac{C_{ref}^2}{2} AL} \tag{18}$$

The dimensionless fluid damping coefficient is thus defined by equation (19). μ_f^* is then plotted as a function of the Strouhal number for three values of the upstream velocity in Figure 10.

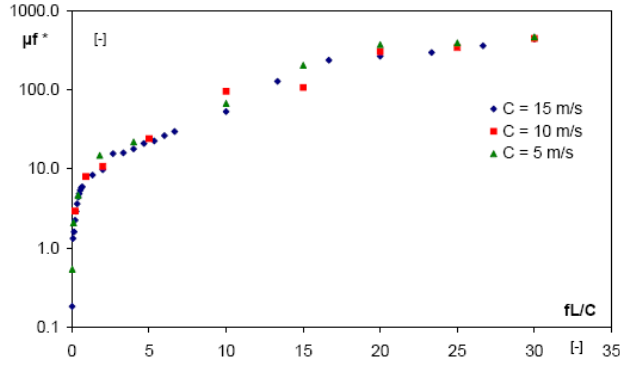$$\mu_f^* = \frac{-\mu_f}{\rho \dfrac{C_{ref}}{2} AL^2} \times 2\pi f \frac{L}{C_{ref}} \tag{19}$$

Figure 10 Dimensionless fluid damping as a function of the frequency for three values of the C_{ref}

The results show that with this normalization, the dimensionless fluid damping for the three values of the upstream velocity fits well. The dependence with the motion frequency is clearly showed. The same result is observed for the dimensionless fluid stiffness coefficient defined by equation (20), see Figure 11.

$$k_f^* = \frac{-k_f}{\rho \dfrac{C_{ref}^2}{2} AL} \times 2\pi f \frac{L}{C_{ref}} \tag{20}$$
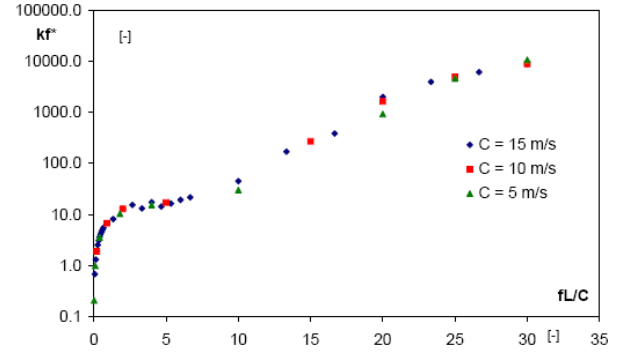

Figure 11 Fluid stiffness as a function of the frequency for three values of the C_{ref}

The hydrodynamic moment can then be evaluated with the model, see equation (25).

$$T_f(C_{ref}, \omega) = -\left[J_f\ddot{\alpha} + \mu_f(C_{ref}, \omega)\dot{\alpha} + k_f(C_{ref}, \omega)\alpha \right] \tag{21}$$

Model assessment

In order to evaluate the model, the case of a free oscillating hydrofoil is considered.

In the free oscillating case, the motion equation of the system, including the hydrofoil, the damper and the structure stiffness, is:

$$J_s\ddot{\alpha} + \mu_s\dot{\alpha} + k_s\alpha = T_f \tag{22}$$

Since the fluid action can be modeled with equation (5), equation (22) can be written as:

$$J_s\ddot{\alpha} + \mu_s\dot{\alpha} + k_s\alpha = -(J_f\ddot{\alpha} + \mu_f\dot{\alpha} + k_f\alpha) \tag{23}$$

$$(J_s + J_f)\ddot{\alpha} + (\mu_s + \mu_f)\dot{\alpha} + (k_s + k_f)\alpha = 0 \tag{24}$$

$$J_e\ddot{\alpha} + \mu_e\dot{\alpha} + k_e\alpha = 0 \tag{25}$$

The diagram of the system in the free oscillating case is presented in Figure 12.

Introducing the pulsation $\omega_o = \sqrt{k_e/J_e}$ and the dimensionless damping coefficient $\xi = \mu_e/\mu_c$ (with the critical damping $\mu_c = 2\sqrt{J_e k_e}$), the canonical form of the differential equation (10) can be written as:

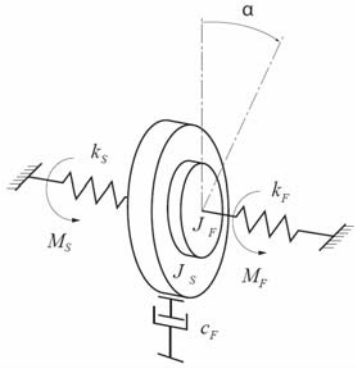$$\ddot{\alpha} + 2\xi\omega_o\dot{\alpha} + \omega_o^2\alpha = 0 \tag{26}$$

Figure 12 Diagram of the fluid structure system

A numerical simulation and a prediction of the motion are considered for a case study described in the first column of Table 5. The upstream velocity is equal to $5 \text{ m} \cdot \text{s}^{-1}$. The dimensionless damping coefficient and the pulsation of the free motion, respectively ξ, ω_o, characterizing the time history of the incidence angle, will be compared.

On one hand, the motion is simulated with ANSYS CXF. ξ, ω_o are extracted through a non-linear least squared method. The analytical solution, of the canonical equation (11), is used to fit the numerical solution. According to the operating conditions, the solution is given by equation (27).

$$\alpha = \alpha_0 e^{-\omega_0 \xi t}\left(\cos(\omega_0\sqrt{1-\xi^2}t) + \frac{\xi}{\sqrt{1-\xi^2}}\sin(\omega_0\sqrt{1-\xi^2}t)\right) \quad (27)$$

The results are given in Table 6.

On the other hand, the time history of the hydrofoil free motion is predicted thanks to the added moment of inertia, fluid damping and fluid stiffness identified in the previous part. Indeed, the dimensionless damping coefficient and the pulsation can be calculated with the equations (28) and (29).

$$\xi = \frac{\mu_F(\omega) + \mu_S}{2\sqrt{(J_F + J_S)(k_F(\omega) + k_S)}} \quad (28)$$

$$\omega_o = \sqrt{\frac{k_F(\omega) + k_S}{J_F(\omega) + J_S}} \quad (29)$$

According to forced oscillating hydrofoil analysis, the added moment of inertia is fixed whereas the fluid damping and stiffness coefficients are dependant on the pulsation. The natural frequency of the system taking into account the added moment of inertia is evaluated:

$$\omega_n = \sqrt{\frac{k_S}{J_F + J_S}} \quad (30)$$

Then the fluid damping and stiffness coefficients are evaluated for this pulsation thanks to the forced oscillating hydrofoil analysis, see Figure 10and Figure 11.

$$\begin{aligned}k_f &= k_f(\omega_n) \\ \mu_f &= \mu_f(\omega_n)\end{aligned} \quad (31)$$

The predicted dimensionless damping coefficient and the pulsation can be calculated:

$$\xi_p = \frac{\mu_F(\omega_n) + \mu_S}{2\sqrt{(J_F + J_S)(k_F(\omega_n) + k_S)}} \quad (32)$$

$$\omega_p = \sqrt{\frac{k_F(\omega_n) + k_S}{J_F + J_S}} \quad (33)$$

The pulsation is first estimated, see equation (33).

$$\omega_n = 283 \text{ rad} \cdot \text{s}^{-1} \quad (34)$$

The fluid damping and stiffness coefficient are then determined, and the equivalent coefficients are calculated, see Table 5 .

Table 5 Hydrofoil and fluid parameters

Hydrofoil parameters	Predicted fluid parameters	Equivalent coefficient
$J_S = 1.10^{-5}$	$J_f = 2.43\ 10^{-6}$	$J_e = 1.243\ 10^{-5}$
$[\text{kg} \cdot \text{m}^2]$	$[\text{kg} \cdot \text{m}^2]$	$[\text{kg} \cdot \text{m}^2]$
$k_S = 0.5$	$k_f = -0.16$	$k_e = 0.34$
$[\text{N} \cdot \text{m}]$	$[\text{N} \cdot \text{m}]$	$[\text{N} \cdot \text{m}]$
$\mu_S = 0$	$\mu_f = 5.8\ 10^{-4}$	$\mu_e = 5.8\ 10^{-4}$
$[\text{kg} \cdot \text{m}^2 \cdot \text{s}^{-1}]$	$[\text{kg} \cdot \text{m}^2 \cdot \text{s}^{-1}]$	$[\text{kg} \cdot \text{m}^2 \cdot \text{s}^{-1}]$

The motion characteristics predicted by the model are given in Table 6.

The prediction of the motion frequency and the dimensionless damping is very close to the numerical simulation: the difference is less than 1%. It shows that the fluid stiffness and the added moment of inertia are well predicted as well as the fluid damping coefficient. The simulated and the predicted time histories of the incidence angle are plotted in Figure 13.

Table 6 Motion characteristics

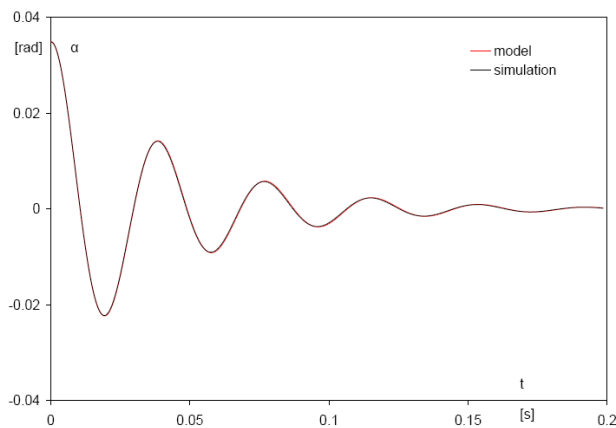| Predicted motion	Simulated of the motion	Difference
$\xi = 0.141$ [–]	$\xi = 0.142$ [–]	less than 1%
$\omega_o = 165$ $\left[\text{rad} \cdot \text{s}^{-1}\right]$	$\omega_o = 165$ $\left[\text{rad} \cdot \text{s}^{-1}\right]$	less than 1%
$f_o = 26.3$ [Hz]	$f_o = 26.4$ [Hz]	less than 1%

Figure 13 Time history of incidence angle: numerical simulation and model.

CONCLUSION

Fluid structure coupling is investigated in the case of an oscillating NACA Hydrofoil. The aim is to identify the flow action in case of vibrating blades in hydraulic machines. This study is a first step to investigate the influence of fluid-structure interactions in turbine or pump system. Numerical simulations of a forced oscillating hydrofoil are carried out to investigate the fluid torque in the frequency domain. The fluid torque on the hydrofoil is identified by a model with three moments: inertial term with an added moment of inertia, a restoring term with a fluid stiffness and a friction action trough a damping coefficient. The three coefficients introduced in the model are identified through an investigation of oscillating hydrofoil in the frequency domain. Then, a simple case of hydro elastic problem is investigated to assess the model: the hydrofoil is attached to a flexible structure featuring a given stiffness and a damper. The structure parameters: moment of inertia, stiffness and damping are fixed. The motion is solution of a second order differential equation. On one hand, the fluid structure interaction problem is solved with ANSYS CFX, on the other hand, the motion is predicted with the model. The comparison shows a very good agreement in terms of pulsation and dimensionless damping which means that the model correctly estimates the fluid damping coefficient as well as the fluid stiffness and the added moment of inertia.

REFERENCES

ANSYS CFX (2005). Solver theory manual, Release 10.0. ANSYS CXF 10.

Belanger F. , Païdoussis M.P. and De Langre E. (1995). "Time-marching analysis of fluid-coupled systems wit large added mass." AIAA Journal **33**(4): 752-757.

Bishop R.E. and Hassan A.Y. (1964). "The Lift and Drag Forces on a Circular Cylinder Oscillating in a Flowing Fluid." Proceedings of the Royal Society of London. Series A, Mathematical and Physical Sciences **277**(1368): 51-75.

Brennen C.E. (1982). A review of added mass and fluid inertial forces, naval civil engineering laboratory.

Carstens V., Kemme R. and Schmitt S. (2003). "Coupled simulation of flow-structure interaction in turbomachinery." Aerospace Science and Technology **7**: 298-306.

Conca C., Osses A. and Planchard J. (1997). "Added mass and damping in fluid-structure interaction." Computer methods in applied mechanics and engineering **146**: 387-405.

Ermanyuk E.V. (2000). "The use of impulse response functions for evaluation of added mass and damping coefficient of a circular cylinder oscillating in linearly stratified fluid." Experiments in Fluids **28**: 152-159.

Gnesin V.I., Kolodyazhnaya L.V. and Rzadkowski R. (2004). "A numerical modelling of stator-rotor interaction in a turbine stage with oscillating blades." Journla of fluids and structures **19**: 1141-1153.

Govardhan R. and Williamson C.H.K. (2000). "Modes of vortex formation and frequency response of a freely vibrating cylinder." Journal of Fluid Mechanics **420**: 85-130.

Han R.P.S. and Xu H. (1996). "A simple and accurate added mass model for hydrodynamic fluid-structure interaction analysis." Journal of Franklin Institute **333B**(6): 929-945.

Jung Y.W. and Park S.O. (2005). "Vortex-shedding characteristics in the wake of an oscillating airfoil at low Reynolds number." Journal of Fluids and Structures **20**: 451-464.

Khalak A. and Williamson C.H.K. (1999). "Motions, Forces and Mode transition in vortex-induced vibrations at low mass-damping." Journal of Fluids and Structures **13**: 813-851.

Khalak A. and Williamson H.K. (1997). "Fluid forced and dynamics of a hydroelastic structure with very low mass and damping." Journal of Fluids and Structures **11**: 973-982.

Launder B.E. and Spalding D.B. (1974). "The numerical computation of turbulent flows." Comput. Methods in Appl. Mech. and Eng **3**(2): 269-289.

Lewin G.C. and Haj-hariri H. (2003). "Modelling thrust generations of a two-dimensional heaving airfoil in a viscous flow." Journal of Fluid Mechanics **492**: 339-362.

Menter F.R. (1994). "Two-equation eddy-viscosity turbulence models for engineering applications." AIAA Journal **32**(8): 1598-1605.

Moffatt S. and He L. (2005). "On decoupled and fully-coupled methods for blade forced response prediction." Journal of Fluids and Structures **20**: 217-234.

Rajasankar J., Iyer N.R. and Appa Rao T.V.S.R (1993). "A new 3-D finite element model to evaluate added mass for analysis of fluid-structure interaction problems." International journal for numerical methods in engineering **36**: 997-1012.

Uchiyama T. (2003). "Numerical prediction of added mass and damping for a cylinder oscillating in confined incompressible gas-liquid two-phase mixture." Nuclear engineering and design **222**: 68-78.

Wilcox D. (1993). "Comparison of two-equation turbulence models for boundary layers with pressure gradient." AIAA Journal **31**(8): 1414-1421.